JOURNAL OF SOLID STATE CHEMISTRY 86, 94–100 (1990)

ESR and Optical Spectroscopy of Ce^{3+} : β''-Alumina

J. D. BARRIE,[1] L. A. MOMODA, AND B. DUNN

Department of Materials Science and Engineering, University of California, Los Angeles, California 90024

AND D. GOURIER, G. AKA, AND D. VIVIEN[2]

Laboratoire de Chimie Appliquee de L'Etat Solide, ENSCP, 11 Rue Pierre et Marie Curie, 75231 Paris Cedex 05, France

Received October 13, 1989

ESR and optical absorption spectroscopy are reported for Ce^{3+} doped β''-alumina and codoped Ce^{3+}–Nd^{3+}–β''-alumina. The doping was achieved by ion exchange techniques. The spectra indicate that the Ce^{3+} ions are found at the mid-oxygen sites in the β''-alumina conduction plane. The g-tensor values were found to be $g_x = 2.58$, $g_y = 2.15$, and $g_z = 0.85$. A small second site occupation (less than 1%) is observed from Ce^{3+} ions located in the Beevers–Ross sites. In the codoped crystals, it is shown that the site occupations of Ce^{3+} and Nd^{3+} ions are not changed when both of these ions are present in the same crystal, an important consideration in energy transfer studies. © 1990 Academic Press, Inc.

1. Introduction

The ability of β''-alumina to incorporate lanthanide and transition metal ions by ion exchange techniques has enabled a variety of luminescent isomorphs to be synthesized (*1, 2*). Among the more interesting optical properties exhibited are laser action and degenerate four-wave mixing shown by Nd^{3+} compositions (*3, 4*) and broadband luminescence demonstrated by Cu^+-doped materials (*5, 6*). Recent work has demonstrated that more than one luminophore can be controllably exchanged into the β''-alumina conduction plane from a single molten salt bath. This synthesis procedure has led to compositions which are capable of producing energy transfer effects, i.e., efficient optical absorption by one ion followed by a transfer of the energy and subsequent luminescence by another ion (*7, 8*). To date, such phenomena have been observed with the sensitizer/activator couples Ce^{3+}/Nd^{3+}, Ce^{3+}/Tb^{3+}, Ce^{3+}/Pr^{3+}, and Yb^{3+}/Er^{3+}. Initial results indicate that the ions are homogeneously distributed in the structure and that the energy transfer $Ce^{3+} \rightarrow Ln^{3+}$ is quite efficient.

One issue which must be addressed in a rigorous approach to energy transfer studies is that of the site occupancies of the various dopant ions. The mechanism of the energy transfer is strongly dependent upon the distance between and the arrangement of the ions between which the transfer

---

[1] Present address: Materials Sciences Laboratory, The Aerospace Corporation M2/241, Los Angeles, CA 90009-2957.

[2] To whom correspondence should be addressed.

0022-4596/90 $3.00

takes place. Optical spectroscopy, ESR, and single crystal X-ray diffraction studies (*9–11*) established that Nd^{3+} ions occupy primarily the mid-oxygen (mO) site in β''-alumina (eightfold coordination, C_{2h} point symmetry). Relatively little occupancy was observed for the four-coordinated (C_{3v} point symmetry) Beevers–Ross (BR) site. Single crystal X-ray studies of Eu^{3+} and Gd^{3+} β''-aluminas show that these lanthanide ions also preferentially occupy the mid-oxygen site (*11*).

This paper reports on the ESR and optical spectroscopy of Ce^{3+}-doped β''-aluminas. The work was performed with the intent of characterizing the site occupation of Ce^{3+} ions exchanged into β''-alumina. The Ce^{3+} ESR results and analyses are much more definitive than the prior work with Nd^{3+} (*9*) and thus provide a better understanding of the ESR response for lanthanide ions in the β''-alumina lattice. In addition, spectroscopy studies of doubly doped Ce^{3+}/Nd^{3+} crystals are presented. These studies are of central importance in establishing whether the process of mixing two ions within the β''-alumina conduction plane leads to any ordering or segregation effects which may affect the energy transfer process.

2. Experimental

Single crystals of Na^+–β''-alumina of starting composition $Na_{1.67}Mg_{0.67}Al_{10.33}O_{17}$ were grown by the flux evaporation techniques (*12*). Ion exchange reactions were used to replace part of the sodium ion content of the crystal with Ce^{3+} or Ce^{3+} and Nd^{3+} by immersing the crystals in eutectic melts of the appropriate chloride salts ($NaCl$, $CeCl_3$, $NdCl_3$) (*7*). Temperatures for the ion exchange process were typically 650°C. The extent of the lanthanide ion exchange was determined by both gravimetric and X-ray absorption analyses (*13*). In the doubly doped materials, the Nd^{3+} content was established independently by measuring the absorption cross section of several of the transitions and comparing this with values determined from singly doped Nd^{3+}–β''-alumina. The Ce^{3+} content was then determined by subtracting the amount of Nd^{3+} from the total amount of exchange as measured from gravimetric and X-ray absorption methods (*7*). The composition of the Ce^{3+}-doped crystals was $Ce_xNa_{1.67-3x}Mg_{0.67}Al_{10.33}O_{17}$, where x ranged from 0.02 to 0.39. The composition of the doubly doped crystals was controlled so that the total lanthanide content was kept constant and only the Ce^{3+}/Nd^{3+} ratio was varied. This resulted in crystals of composition $Ce_yNd_{0.31-y}Na_{0.74}Mg_{0.67}Al_{10.33}O_{17}$, where y was in the range 0.02 to 0.29.

Optical absorption measurements were made over the temperature range 4 to 300 K using an Oxford Instruments cryostat in a Beckman 5270 UV Spectrometer. Optical excitation and emission spectra were measured using a Spex Fluorolog Model F112A spectrofluorometer over the temperature range 77 to 300 K.

The ESR measurements were made at X band using a Bruker 220D spectrometer equipped with an Oxford Instruments helium flow cryostat. The data were acquired at 20 K due to the short spin lattice relaxation time of the Ce^{3+} ion.

3. Results and Discussion

3.1 Electron Spin Resonance

The $^2F_{5/2}$ ground state of trivalent cerium in fields of lower than cubic symmetry is split into three Kramers doublets (*14*). The splitting is generally such that only the lowest doublet is populated and the system can be treated as for an effective spin $S = 1/2$. Thus, ESR transitions occur at a magnetic field, B_0, given by $h\nu = g\beta B_0$, where $h\nu$ is the microwave energy, β is the Bohr magneton, and g is given by

$$g^2 = (lg_x)^2 + (mg_y)^2 + (ng_z)^2,$$

where l, m, and n are the direction cosines of the field B_0 with respect to the g-tensor axes.

Figure 1 shows two representative ESR spectra recorded with the magnetic field B_0 parallel and perpendicular to the crystallographic c axis in a Ce^{3+}-doped β''-alumina single crystal of composition $Ce_{0.31}Na_{0.75}Mg_{0.67}Al_{10.33}O_{17}$. For $B_0 \| c$, the spectrum exhibits a strong, broad line at $g = 2.58$ with linewidth $\Delta B = 39$ mT and a weak line at $g = 4.16$ with $\Delta B = 11$ mT (Fig. 1a). The intensity of the weak line (measured by $s(\Delta B)^2$, where s is the peak to peak height of the line) is only 1% of that of the broad line. By rotating the magnetic field from the c axis to the basal plane (Fig. 2), the broad line splits into three components while the weak line remains unsplit and shifts rapidly to high field. This weaker line is only detectable when the angle between the c axis and B_0 is less than 50° (triangles in Fig. 2). This dissimilar behavior indicates that the two lines arise from two different Ce^{3+} species in the material. A second indication that the weak line belongs to a different species than does the broad line is that its lifetime broadening occurs at a lower temperature than that of the broad line (60 versus 100 K). The rotation of B_0 in the basal plane produces only the broad lines (Fig. 1b). The angular variation of these broad lines exhibits a 60° periodicity (Fig. 3), indicating that the Ce^{3+} ions occupy three crys-

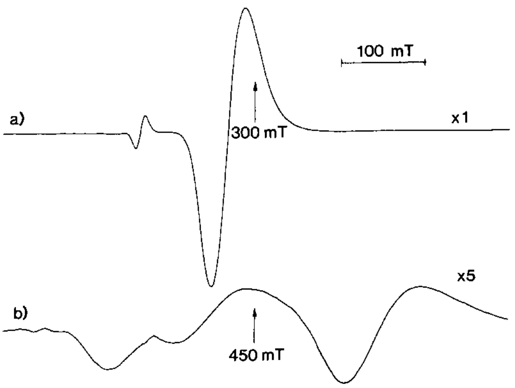

FIG. 1. Representative ESR spectra at 20 K of Ce^{3+} ion exchange β''-alumina with (a) $B_0 \| c$ and (b) $B_0 \perp c$, at 15° from the a axis ($Ce_{0.31}Na_{0.75}Mg_{0.67}Al_{10.33}O_{17}$).

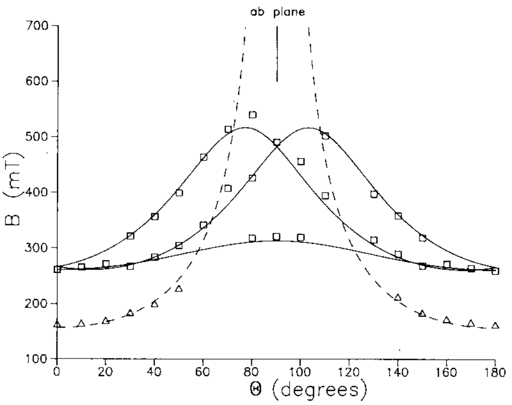

FIG. 2. Angular variation of the ESR signal for Ce^{3+} ion exchange β''-alumina. The applied magnetic field B_0 is in a plane containing the c axis. The triangles and squares are experimental data for the weak and broad lines, respectively. Dotted lines are calculated for a purely $|5/2, \pm 5/2>$ fundamental Kramers doublet. Solid lines are calculated for the Kramers doublet given by Eq. (4) with $p = 0.13$, $q = 0.955$, and $r = 0.045$ and assuming a deviation of the g_x axis by 13° from the c axis.

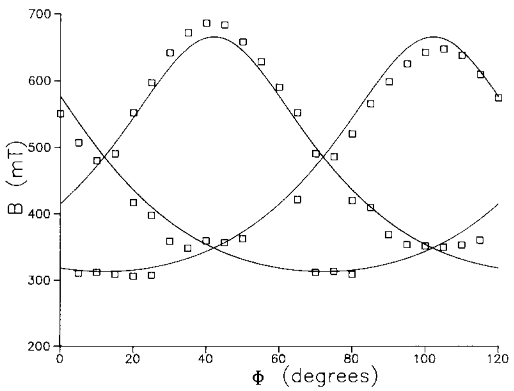

FIG. 3. Angular variation of the ESR signal for Ce^{3+} ion exchange β''-alumina. The applied magnetic field B_0 is in the ab (basal) plane. The solid lines are calculated for the Kramers doublet given by Eq. (4) with $p = 0.13$, $q = 0.955$, and $r = 0.045$ and assuming a deviation of the g_x axis by 13° from the c axis.

tallographically equivalent sites with low symmetry. This behavior is comparable to that observed with Nd^{3+}-exchanged β''-alumina (*9*).

The angular variation of the broad line spectrum in both orientations is best fit using the following g values (± 0.01): $g_x = 2.58$, $g_y = 2.15$, $g_z = 0.85$, with the y axis of the g tensor in the crystallographic ab plane and the x axis of the g tensor deviating from the crystallographic c axis by $\varepsilon = 13°$. The effect of this site splitting is evident in the angular variation of the ESR spectrum from the c axis to the basal plane (solid lines in Fig. 2) where the highest field for the ESR transition occurs at 13° from the ab plane. The fit of the angular variation is very sensitive to the tilt angle ε. The experimental g values for this site with low symmetry can be understood by considering the electronic ground state of Ce^{3+} ions.

For a Ce^{3+} ion in a $^{2S+1}L_J = {}^2F_{5/2}$ state, the two components $|\alpha>$ and $|\beta>$ of a Kramers doublet may be expressed as linear combinations of states of different magnetic quantum number $M = \pm 5/2, \pm 3/2, \pm 1/2$ corresponding to $J = 5/2$, i.e.,

$$|\alpha> = \sum_M a_M |J, M>$$
$$|\beta> = \sum_M (-1)^{2M} a_M^* |J, -M>, \qquad (1)$$

where a_M^* is the complex conjugate of a_M and the values of M in the summation are determined by the symmetry of the cerium sites. In a C_{3h} symmetry (which is a higher symmetry than is observed at either site in the β''-alumina conduction plane) the crystal field splits the $^2F_{5/2}$ ground state to give three Kramers doublets $|5/2, \pm M>$ for which the following g values are expected (*14*)

$$\begin{aligned} |5/2, \pm 1/2> \quad & g_\parallel = 6/7 = 0.86 \\ & g_\perp = 18/7 = 2.57 \\ |5/2, \pm 3/2> \quad & g_\parallel = 18/7 = 2.57 \\ & g_\perp = 0 \\ |5/2, \pm 5/2> \quad & g_\parallel = 30/7 = 4.29 \\ & g_\perp = 0, \end{aligned} \qquad (2)$$

where $g_\parallel$ is the g tensor value in the direction of the C_3 axis and $g_\perp$, the value perpendicular to this axis. Lowering of the symmetry further may result in modification of these values, and the splitting of the $g_\perp$ into two independent g factors as discussed below.

There is good agreement between the experimental and expected values for $g_\parallel$ and $g_\perp$. If one takes $g_\parallel = g_z = 0.85$ and $g_\perp = 1/2(g_x + g_y) = 2.37$, the resulting values are close to the ones expected for a purely $|5/2, \pm 1/2>$ ground state ($g_\parallel = 0.86$ and $g_\perp = 2.57$). The orthorhombic g tensor and the existence of three crystallographically equivalent sites indicates that this site corresponds to the mO position in the conduction plane. The symmetry of the mO site is C_{2h} with the C_2 axis parallel to the a crystallographic axis, which implies a $g_z(g_\parallel)$ direction perpendicular to the c axis. Experimentally, however, the z axis of the g tensor is found at 13° from the basal plane. This behavior could be related to the structural nature of the β''-alumina conduction plane. In β''-alumina, the conduction plane is not a mirror plane. Instead, the plane possesses a "zigzag" character with the BR sites representing the maximum distances above and below the center line of the conduction plane at the mO site. Ions situated in the mO sites are thus subject to an asymmetric perturbation due to ions found in nearby BR sites (*15*). It is interesting to note that the angle between the center of the mO site and the BR sites above and below the mO site is approximately 11°.

The low symmetry of the mO sites induces an admixture of the lowest lying Kramers doublets. In twofold symmetry such as that found at the mO site, the crystal field admixes states with M values differing by 2. The fundamental Kramers doublet is not purely $|5/2, \pm 1/2\rangle$, but has the form (*16*)

$$|{}^{\alpha}_{\beta}\rangle = p|5/2, \pm 5/2\rangle + q|5/2, \pm 1/2\rangle + r|5/2, \mp 3/2\rangle, \quad (3)$$

where p, q, and r are the fraction of each component contributing to the ground state. This combination gives the following g values:

$$\begin{aligned} g_x &= \pm(6/7)(2\sqrt{5}pr + 4\sqrt{2}qr + 3q^2) \\ g_y &= \pm(6/7)(2\sqrt{5}pr - 4\sqrt{2}qr + 3q^2) \quad (4) \\ g_z &= \pm(6/7)(5p^2 + q^2 - 3r^2). \end{aligned}$$

From the experimental results, it is expected that $q \gg p, r$ (i.e., the ground state is primarily $|5/2, \pm 1/2\rangle$), with the coefficient r being responsible for the orthorhombicity of the g tensor. For example, taking $p = 0.13$, $q = 0.955$, and $r = 0.045$, the calculated values, $|g_x| = 2.58$, $|g_y| = 2.16$, and $|g_z| = 0.85$, are extremely close to the experimental ones. This agreement between experimental and calculated g values indicates that the ESR signal corresponding to 99% of the Ce^{3+} ions originates from ions occupying the mO site of the conduction plane.

The weak line spectrum is consistent with that expected for Ce^{3+} in a site with axial symmetry. The fact that this line does not split upon rotation from the c axis, and is not observable when B_0 lies in the basal plane, indicates that the corresponding Ce^{3+} ions occupy an axial site with $g_{\|} > 2$ and $g_{\perp} \ll 2$. The weak line can, therefore, be assigned to Ce^{3+} ions in the BR sites of the conduction plane, which have C_{3v} symmetry and $C_3 \| c$.

The experimental results, which give $g_{\|} = 4.16$, strongly suggest that the ground state in the BR site is $|5/2, \pm 5/2\rangle$ [cf. Eq. (2)]. The theoretical angular variation for this Kramers doublet (dotted line in Fig. 2) fits reasonably well with the experimental data available for $\Theta < 50°$. In the BR site, which is an axially distorted tetrahedral site, there is no inversion center and the crystal field admixes states with M values which differ by 3. Thus the two components of the fundamental Kramers doublet should be

$$|{}^{\alpha}_{\beta}\rangle = p|5/2, \pm 5/2\rangle + q|5/2, \mp 1/2\rangle, \quad (5)$$

and the $g_{\perp}$ value, given by $g_{\perp} = (18/7)q^2$, should differ slightly from zero. Unfortunately, the data for B_0 lying in the basal plane could not be resolved, probably because the line is too weak and too broad to be detectable, and it was, therefore, not possible to determine the amount of mixing between the $|5/2, \pm 5/2\rangle$ and $|5/2, \pm 1/2\rangle$ states (i.e., the values of p and q for this site). Nevertheless, the ESR data for this weak line ESR spectrum are clearly consistent with the assignment of the Ce^{3+} ion to the BR site.

In a crystal containing both Ce^{3+} and Nd^{3+} (with composition $Ce_{0.16}Nd_{0.16}Na_{0.75}Mg_{0.67}Al_{10.33}O_{17}$), the ESR spectrum for the Ce^{3+} ions is identical to that of the singly doped crystals. For $B_0 \| c$, the Ce^{3+} spectrum contains the weak line attributed to Ce^{3+} ions in BR sites as well as the strong broad peaks which arise from Ce^{3+} in mO sites. This spectrum indicates that the presence of Nd^{3+} ions in the conduction plane has no effect upon the site distribution of the Ce^{3+} ions.

3.2 Optical Spectroscopy

Optical absorption measurements of single crystals of β''-alumina ion exchanged with Ce^{3+} show the $4f$–$5d$ interconfigurational transitions characteristic for this ion. For dilute samples, four bands were observed in the spectra at 233, 267, 297, and 332 nm (Fig. 4). It was not possible to observe absorption spectra for crystals containing more than 2×10^{20} ions/cm^3 (corresponding to $Ce_{0.06}$) due to the high oscillator

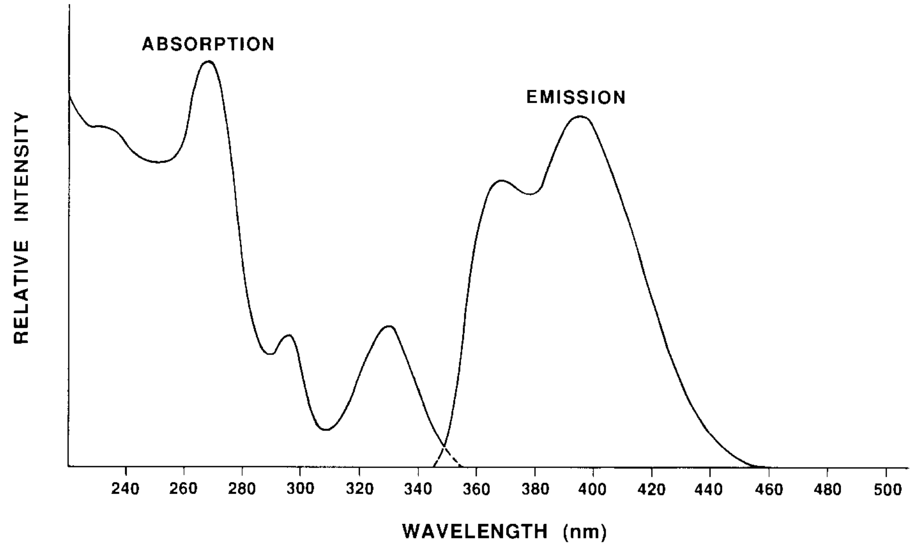

FIG. 4. Optical absorption/emission spectrum of Ce^{3+} ion exchange β''-alumina ($Ce_{0.06}Na_{1.49}Mg_{0.67}Al_{10.33}O_{17}$). The absorption spectrum was measured at 4 K, while the emission was measured at 77 K.

strength of the Ce^{3+} absorption bands. Optical excitation spectra recorded using the 400-nm Ce^{3+} emission confirmed the presence of four distinct bands in the region 200 to 350 nm for samples containing as much as 1×10^{21} ions/cm^3. The splitting of the 5*d* excited state into multiple bands is common for Ce^{3+} ions found in sites of low symmetry (*17*), and is expected for the mid-oxygen site in the conduction plane of β''-alumina.

The emission spectra of the Ce^{3+}-doped β''-alumina crystals exhibited the distinct two-peaked band originating from transitions from the 5*d*-excited state to the spin-orbit split $4f^1$ ground state (*7*). The degree of this splitting is in good agreement with the splitting of the 4*f* band observed by infrared absorption spectra (not shown here).

The optical absorption at 4 K for samples containing both Ce^{3+} and Nd^{3+} was measured. The absorption spectrum for the Ce^{3+} ions was unchanged, and that observed for the Nd^{3+} was identical to spectra obtained for Nd^{3+}-doped samples. It is interesting to note that in a sample containing 0.9×10^{20} Ce^{3+} ions/cm^3 and 9×10^{20} Nd^{3+} ions/cm^3 ($Ce_{0.03}Nd_{0.28}Na_{0.84}Mg_{0.67}Al_{10.33}O_{17}$), only one absorption line was observed for the $^4I_{9/2} \rightarrow {}^2P_{1/2}$ transition of neodymium (at 427 nm). Because the $^2P_{1/2}$ state is not split by spin-orbit coupling and only the lowest Stark level of the $^4I_{9/2}$ shell is populated at this temperature, the single line indicates that the Nd^{3+} occupies only the mid-oxygen site in this crystal. In samples containing only Nd^{3+} (*9*), there was some occupancy of the BR site; however, in mixed Ce^{3+}/Nd^{3+} compositions no such BR occupancy for Nd^{3+} is evident. The absorption spectra for the mixed compositions also contain no lines which suggest the presence of Nd^{3+} ion pairs. In summary the absorption spectra for mixed Ce^{3+}/Nd^{3+}–β''-alumina are representative of isolated Ce^{3+} and Nd^{3+}, with each ion located predominantly, if not exclusively, on the mid-oxygen site.

4. Summary

The ESR spectra for Ce^{3+}-doped β''-alumina single crystals clearly show that the cerium ions reside primarily in the mid-oxygen site of the conduction plane. The angular variation in the *ab* plane gives the behavior expected for Ce^{3+} ions in mO sites characterized by C_{2h} symmetry. The tilting of the magnetic axes away from the crystalline axes may be related to the asymmetric arrangement of ions about the mO site. In addition to the population of the mO site, there is a small (1%) occupancy of the BR site.

In crystals containing both Ce^{3+} and Nd^{3+}, the Ce^{3+} spectra are unchanged and the Nd^{3+} spectra are identical to those of Nd^{3+}-doped crystals. There is no indication that site occupancies for Ce^{3+} or Nd^{3+} are altered because of the presence of the other lanthanide ion. This behavior is not surprising in view of the similarity in ionic size and the large number of mid-oxygen sites available in the conduction plane. For example, samples containing $\sim 1 \times 10^{21}$ lanthanides/cm^3 (55% exchange) will fill less than one-third (5/27) of the available mid-oxygen sites.

The studies reported here are important for determining the ion interactions involved in energy transfer. The presence of lanthanides in identical sites and the absence of detrimental segregation effects provide important crystal chemical explanations why the β''-aluminas exhibit excellent energy transfer.

Acknowledgments

The research was supported by the U.S. Office of Naval Research, NATO collaborative Grant No. 890337, and by the Franco-American Commission for Cultural Exchange. The authors thank Professor E. Wong for his insightful review of the manuscript and D. Simons for experimental assistance.

References

1. G. C. Farrington, B. Dunn, and J. O. Thomas, *Appl. Phys. A* **32,** 159 (1983).
2. B. Dunn and G. C. Farrington, *Solid State Ionics* **18/19,** 31 (1986).
3. M. Jansen, A. Alfrey, O. M. Stafsudd, B. Dunn, D. L. Yang, and G. C. Farrington, *Opt. Lett.* **9,** 119 (1984).
4. R. W. Boyd *et al., Opt. Lett.* **11,** 162 (1986).
5. J. D. Barrie, B. Dunn, O. M. Stafsudd, and P. Nelson, *J. Lumin.* **37,** 303 (1987).
6. J. D. Barrie, B. Dunn, G. Hollingsworth, and J. I. Zink, *J. Phys. Chem.* **93,** 3958 (1989).
7. L. A. Momoda, J. D. Barrie, and B. Dunn, *Mater. Res. Bull.* **24,** 859 (1989).
8. L. A. Momoda, J. D. Barrie, B. Dunn, and O. M. Stafsudd, "Proceedings of the Electrochemical Society Symposium on Luminescence Science and Technology" (C. W. Struck, B. DiBartolo, and W. M. Yen, Eds.), 88-24, p. 235 (1989).
9. B. Dunn, D. L. Yang, and D. Vivien, *J. Solid State Chem.* **73,** 235 (1988).
10. A. Alfrey, O. M. Stafsudd, B. Dunn, and D. L. Yang, *J. Phys. Chem.* **88,** 707 (1988).
11. W. Carrillo-Cabrera, J. O. Thomas, and G. C. Farrington, *Solid State Ionics,* **28–30,** 317 (1988).
12. J. L. Briant and G. C. Farrington, *J. Solid State Chem.* **33,** 385 (1980).
13. J. Tegenfeldt, M. Underwood, and G. C. Farrington, *Solid State Ionics* **18/19,** 668 (1986).
14. A. Abragam and B. Bleaney, "Electron Paramagnetic Resonance of Transition Ions," p. 308ff, Oxford Univ. Press (Clarendon), London/New York (1970).
15. M. Bettman and C. R. Peters, *J. Phys. Chem.* **73,** 1774 (1969).
16. S. D. McLaughlan and P. A. Forrester, *Phys. Rev.* **151,** 311 (1966).
17. G. Blasse, "Handbook on the Physics and Chemistry or Rare Earths" (K. A. Gschneidner and L. Eyring, Eds.), p. 237, North-Holland, Amsterdam (1979).